

The impact of latent confounders in directed network analysis in neuroscience

Rebecca Ramb, Michael Eichler, Alex Ing, Marco Thiel, Cornelius Weiller, Celso Grebogi, Christian Schwarzbauer, Jens Timmer and Björn Schelter

Phil. Trans. R. Soc. A 2013 **371**, 20110612, published 15 July 2013

References

This article cites 37 articles, 2 of which can be accessed free
<http://rsta.royalsocietypublishing.org/content/371/1997/20110612.full.html#ref-list-1>

Subject collections

Articles on similar topics can be found in the following collections

[graph theory](#) (2 articles)
[medical physics](#) (17 articles)

Email alerting service

Receive free email alerts when new articles cite this article - sign up in the box at the top right-hand corner of the article or click [here](#)

Research



Cite this article: Ramb R, Eichler M, Ing A, Thiel M, Weiller C, Grebogi C, Schwarzbauer C, Timmer J, Schelter B. 2013 The impact of latent confounders in directed network analysis in neuroscience. *Phil Trans R Soc A* 371: 20110612. <http://dx.doi.org/10.1098/rsta.2011.0612>

One contribution of 13 to a Theme Issue 'Assessing causality in brain dynamics and cardiovascular control'.

Subject Areas:

medical physics, graph theory

Keywords:

Granger causality, renormalized partial directed coherence, vector autoregressive modelling, latent confounders

Author for correspondence:

Björn Schelter

e-mail: schelter@fdm.uni-freiburg.de

[†]Present address: Department of Diagnostic Radiology, Medical Physics, University Hospital Freiburg, Breisacher Strasse 60a, 79106 Freiburg, Germany.

The impact of latent confounders in directed network analysis in neuroscience

Rebecca Ramb^{1,†}, Michael Eichler², Alex Ing³, Marco Thiel⁴, Cornelius Weiller⁵, Celso Grebogi^{4,6}, Christian Schwarzbauer³, Jens Timmer^{1,6,7,8} and Björn Schelter^{1,4,5,7,9}

¹FDM, Freiburg Center for Data Analysis and Modeling, University of Freiburg, Eckerstrasse 1, 79104 Freiburg, Germany

²Department of Quantitative Economics, Maastricht University, PO Box 616, 6200 MD Maastricht, The Netherlands

³Aberdeen Biomedical Imaging Centre, University of Aberdeen, Aberdeen AB25 2ZD, UK

⁴Institute for Complex Systems and Mathematical Biology, SUPA, University of Aberdeen, Aberdeen AB24 3UE, UK

⁵Department of Neurology, Center for Neuroscience, University Hospital Freiburg, Breisacherstrasse 64, Freiburg 79106, Germany

⁶Freiburg Institute for Advanced Studies (FRIAS), University of Freiburg, Albertstrasse 19, 79104 Freiburg, Germany

⁷Department of Physics, University of Freiburg, Hermann-Herder-Strasse 3, 79104 Freiburg, Germany

⁸Department of Clinical and Experimental Medicine, Linköping University, 58183 Linköping, Sweden

⁹Division of Functional Brain Imaging (FBI), Department of Neurology, University Medical Center of Freiburg, Breisacher Strasse 64, 79106 Freiburg, Germany

In the analysis of neuroscience data, the identification of task-related causal relationships between various areas of the brain gives insights about the network of physiological pathways that are active during the task. One increasingly used approach to identify causal connectivity uses the concept of Granger causality that exploits predictability of activity in one region by past activity in other regions of the brain. Owing to the complexity of the data,

selecting components for the analysis of causality as a preprocessing step has to be performed. This includes predetermined—and often arbitrary—exclusion of information. Therefore, the system is confounded by latent sources. In this paper, the effect of latent confounders is demonstrated, and paths of influence among three components are studied. While methods for analysing Granger causality are commonly based on linear vector autoregressive models, the effects of latent confounders are expected to be present also in nonlinear systems. Therefore, all analyses are also performed for a simulated nonlinear system and discussed with regard to applications in neuroscience.

1. Introduction

An increasing number of studies based on, for instance, electroencephalography (EEG), magnetoencephalography (MEG), near-infrared spectroscopy (NIRS) or functional magnetic resonance imaging (fMRI) use complex data analysis methods to investigate the functional architecture of the brain [1–5]. These novel methods analyse the internal ‘communication’ networks of the brain based on functional connectivity [6–10]. For a better understanding of the results of such connectivity analyses, the inferred networks are often visualized by graphs in which recorded time series indicating activity of certain brain regions are represented by nodes, whereas dependences among the time series are encoded by edges linking the nodes. Depending on the type of analysis, such edges can be undirected (lines) for undirectional associations or directed (arrows) for directional associations. In the context of EEG, MEG, NIRS and fMRI, both—undirected and directed—types of connectivity measures are commonly applied. Most studies, however, comprise undirected analyses, for an overview, see Smith *et al.* [11].

The ultimate goal of connectivity analyses is the identification of physiological pathways that, for instance, transport information between brain regions. Therefore, one further step in the analysis of interrelations is the investigation of causal relationships. Although there is no clear universally accepted definition of causality, several concepts for causality that provide a suitable framework for causal inference have been proposed; for a general overview, we refer to [12,13] and particularly in the context of multiple time series, we refer to [14,15]. In the context of time series and neuroscience, there are various recent works in the broader context of causality [16–18]. This study deals with Granger causality [19–21], which provides an increasingly used measure to investigate causal interrelations. In the case of fMRI, causality assertions have to be treated with caution because haemodynamic responses do not cause haemodynamic responses. However, simulation studies revealed that Granger causality analyses still provide information about the underlying network structure for fMRI data [22,23]. The derived graphical representations in this study contain vertices referring to the acquired time-series data and edges that are defined in terms of Granger causality, hence are directed. This kind of graph is then referred to as a Granger causality graph [2,24,25].

In particular, with regard to statistical inference, causality is challenging because finite numbers of correlations are used to draw conclusions about overall causal interrelations. In neuroscience analyses, often regions of interest are established or imposed by placement of the electrodes, before further investigations of causal connections follow. For instance, in non-invasive EEG, hidden sources in the brain may be the cause for the acquired data at the scalp electrodes. The severe effect of displaced electrodes in this case was emphasized in [26], where the issue of assuming one sensor per source is addressed. So, on the one hand, constraints on the regions restrict the complexity of the analysis, but on the other hand, restrictions contain previous determination of relevance of components within the analysis. The investigation of directed connections is biased from the beginning.

Missing important components in the network, aggregation over spatial information and over time leads to an identification of components that allow latent influences to disturb deriving

overall causalities. Unforeseen causality assertions therefore occur. Which kind of causality structure is present then depends on the components that are included in the network analysis, and statements about causality tend to become uncertain.

In this study, unobserved components, which provide influence structures in the network, but which are excluded from the analysis, are called latent confounders. Other attempts to investigate latent confounders are given, for instance, in the context of partial Granger causality [27] or in showing the need to account for the effect of latent sources, as was done in [28] for cardiovascular variability series. Further, the algorithm for inductive causation with latent variables [29] was introduced to find invariant substructures based on equivalent graphs. However, errors owing to accidental correlations may occur [30].

The investigations in this paper demonstrate how latent confounders, which form intermediate vertices in directed paths of Granger causality graphs, lead to additional direct relations and to further spurious relations between other components. Three specific types of influence paths are studied in order to detect paths that can be confirmed in Granger causality analyses. Because bivariate Granger causality analysis, as presented in [2], naturally reflects the effect of latent confounders in subsystems, a combination of bivariate and multivariate analyses is applied in simulations to provide further information about spurious causalities.

When dealing with the human brain, the underlying system will be nonlinear. In neuroscience, the investigations of the effects of latent confounders thus cannot be restricted to the linear case. We therefore provide a simulation in the nonlinear case as well. As a statistical tool to detect Granger causalities, and thus edges in Granger causality graphs, we choose renormalized partial coherence [31], which is a further development of partial directed coherence (PDC) [32,33].

This paper is organized according to the following structure. First, a background in vector autoregressive (VAR) modelling as well as the concept of Granger causality are introduced, and the notion of renormalized PDC is briefly discussed. Second, the effects of latent confounders are illustrated in a simulated linear system based on a VAR model, and a system of four coupled Roessler systems, to study the effect of latent confounders in nonlinear systems. Subsequently, three types of influence paths are studied for both types of systems, and the combination of bivariate and multivariate analyses is considered. Finally, the initially demonstrated effect of a latent confounder is discussed with respect to applications.

2. Granger causality in vector autoregressive modelling

Underlying concepts and methods are briefly explained. Further details on VAR modelling and Granger causality can be found in [34–36].

(a) Granger causality

The concept of Granger causality [19–21] provides operational definitions for causality relations and interactions in empirical investigations. The concept is based on the assumption that causes always precede their effects, that causal relationships remain constant and that all relevant variables are included in the evaluation. In particular, on account of non-observance of the latter assumption, numerous spurious statements in the determination of causal influences occur.

The concept is rooted in probabilistic considerations, where the assumptions above are expressed based on stochastic processes. Hence, let X_V be a $|V|$ -dimensional stationary stochastic process with its d components indicated by the set $V = \{1, \dots, d\}$. Individual components may then be referred to by X_1, X_2, \dots, X_d . Component X_1 is Granger causal for X_2 , if previous outcomes of X_1 improve the prediction of present outcomes of X_2 . Improvement means the prediction error is less, i.e. the mean square error decreases if the causing component is included, and directed causal influences are then captured as the effect of reduction of the variance of the prediction error.

Owing to operational limitations, the number of components included in Granger causality considerations is necessarily restricted. Causality assertions therefore require declaration of the

set of components included in the analysis, which means that not the ‘whole universe’ is considered as suggested by Granger [19]. The Granger causal influence from component X_1 to component X_2 , given the set of components in the stochastic process X_V , can be expressed as

$$X_1 \rightarrow X_2 | X_V. \quad (2.1)$$

For theoretical reasons, inference of causality would actually require the consideration of all subsystems. The concept of Granger causality with respect to linear influences becomes apparent in VAR models, which in addition form the foundation for the renormalized PDC.

(b) Vector autoregressive processes

VAR processes represent multi-dimensional stochastic processes for which outcomes linearly emerge from past values. Let X_V be again a $|V|$ -dimensional stationary stochastic process with d components. Moreover, assume that X_V possesses a VAR representation such that

$$X_V(t) = \sum_{u=1}^p A(u)X_V(t-u) + \varepsilon_V(t), \quad t \in \mathbb{Z}, \quad (2.2)$$

where $\{A(u)\}_{u=1,\dots,p}$ is a sequence of real-valued $|V| \times |V|$ matrices and $\{\varepsilon_V(t), t \in \mathbb{Z}\}$ is a Gaussian white noise process consisting of $|V| \times 1$ vectors. The covariance matrix of the noise process is denoted by $\Sigma = (\sigma_{mn}^2)_{m,n \in \{1,\dots,d\}}$.

For a VAR model of order p , the best linear predictor $\hat{X}_V(t | t-1)$ with respect to the past of all other components is obtained by

$$\hat{X}_V(t | t-1) = \sum_{u=1}^p A(u)X_V(t-u). \quad (2.3)$$

The variance of the error in the prediction of the i th component at time t is then given by

$$\text{var}[X_i(t) - \hat{X}_i(t | t-1)] = \text{var}[\varepsilon_i(t)] = \sigma_{ii}^2. \quad (2.4)$$

To test whether another component $X_j, j \neq i$, has a Granger causal impact on the outcome of $X_i(t)$, compute the variance in the prediction error without the information of past values of X_j . Because the process X_V provides a VAR representation, the subprocess $X_{V \setminus \{j\}}$, i.e. the same process but without the j th component, possesses such a representation as well [35], i.e.

$$X_{V \setminus \{j\}}(t) = \sum_{u=1}^{\infty} B(u)X_{V \setminus \{j\}}(t-u) + \eta_{V \setminus \{j\}}(t), \quad t \in \mathbb{Z}, \quad (2.5)$$

where $\{B(u)\}_{u=1,\dots,p}$ is a sequence of real-valued $(|V|-1) \times (|V|-1)$ matrices, and $\{\eta_{V \setminus \{j\}}(t), t \in \mathbb{Z}\}$ is a Gaussian white noise process. Moreover, the covariance matrix of the noise process is recalculated and given by some $\tilde{\Sigma} = (\tilde{\sigma}_{mn}^2)_{m,n \in \{1,\dots,d\}}$. Analogously, the variance of the prediction error of the i th component is calculated. In the smaller model $X_{V \setminus \{j\}}$, the result is given by

$$\text{var}[X_i(t) - \hat{X}_i(t | t-1)] = \text{var}[\eta_i(t)] = \tilde{\sigma}_{ii}^2. \quad (2.6)$$

Here, the equation consists of $(|V|-1)$ -dimensional vectors. Following the conceptual idea of Granger causality, the comparison of σ_{ii}^2 and $\tilde{\sigma}_{ii}^2$ is used to detect causal influence. Equality indicates absence of linear Granger causal influence,

$$X_j \nrightarrow X_i | X_V \Leftrightarrow \sigma_{ii}^2 = \tilde{\sigma}_{ii}^2. \quad (2.7)$$

If all autoregressive coefficients $A_{ij}(u)$ are zero for every $u \in \{1, \dots, p\}$, then the i th entries in all vectors of both Gaussian white noise processes are the same, and therefore, independent of

whether the information of X_j is included or not. Thus, Granger causalities become apparent in the autoregressive coefficients

$$X_j \rightarrow X_i | X_V \Leftrightarrow A_{ij}(u) = 0, \quad \text{for all } u \in \{1, \dots, p\}, \text{ for } i \neq j. \quad (2.8)$$

(c) Renormalized partial directed coherence

The concept of detecting Granger non-causalities by zero autoregressive coefficients is also realized as a statistical tool in the frequency domain called PDC [32,33] and its further development as renormalized PDC (rPDC) [31]. Here, the rPDC is used to infer Granger causality for time-series data, and the main notions for statistical inference are listed below.

Transition to the frequency domain is performed by Fourier transforming the autoregressive coefficients, which are further split into real and imaginary parts component by component,

$$\mathbf{A}_{ij}^{\text{split}}(\lambda) := \begin{pmatrix} \text{Re}[\mathbf{A}_{ij}(\lambda)] \\ \text{Im}[\mathbf{A}_{ij}(\lambda)] \end{pmatrix}, \quad \text{where } \mathbf{A}(\lambda) := \mathbf{1} - \sum_{u=1}^p A(u) e^{-i\lambda u}. \quad (2.9)$$

Using the covariance matrix of the estimator $\hat{\mathbf{A}}_{ij}^{\text{split}}(\lambda)$, i.e.

$$V_{ij}(\lambda) := \sum_{k,l=1}^p H_{ij}(k,l) \Sigma_{ii} \begin{pmatrix} \cos(k\lambda) \cos(l\lambda) & \cos(k\lambda) \sin(l\lambda) \\ \sin(k\lambda) \cos(l\lambda) & \sin(k\lambda) \sin(l\lambda) \end{pmatrix}, \quad (2.10)$$

where $H(k,l)$ denotes the inverse of the covariance matrix of the VAR process, Granger causality in the frequency domain is inferred via estimating the rPDC value obtained by

$$\text{rPDC}_{ij}(\lambda) = (\hat{\mathbf{A}}_{ij}^{\text{split}}(\lambda))^t (\hat{V}_{ij})^{-1}(\lambda) \hat{\mathbf{A}}_{ij}^{\text{split}}(\lambda). \quad (2.11)$$

Thus, estimation of the rPDC requires estimators for the matrices H , Σ and $A(u)$. Through the renormalization, a constant critical value is obtained, as shown in [31].

(d) Networks and graphs

A graph G is an abstract object that consists of two sets: a set of vertices V and a set of edges E . In graphical modelling, graphs are used in combination with probability theory [37], and inference of graphs in the context of time-series analysis was first introduced by Dahlhaus [38], with further developments by Eichler [24]. In this study, single vertices correspond to single series of time-series data, and edges reflect Granger causalities. In terms of the stochastic process X_V , the corresponding graph then contains vertices $1, \dots, d$ referring to the components X_1, \dots, X_d , and a directed edge from X_a to X_b , i.e. $a \rightarrow b$, if $X_a \rightarrow X_b | X_V$. The frequency domain tool of renormalized PDC is used to determine directed edges between pairs of vertices in the graph.

3. Effects of latent confounders

In this section, effects of unobserved components in the connectivity analysis of direct directed interaction are illustrated. The influence of latent confounders is first demonstrated in a linear stochastic system, then in a nonlinear system.

(a) Analysis of a linear stochastic system

To demonstrate the spurious detection of additional edges, we investigate the following four-dimensional VAR process, as suggested in [2],

$$\left. \begin{aligned} X_1(t) &= \alpha X_4(t-2) + \varepsilon_1(t), & X_3(t) &= \varepsilon_3(t), \\ X_2(t) &= \beta X_4(t-1) + \gamma X_3(t-1) + \varepsilon_2(t) \quad \text{and} & X_4(t) &= \varepsilon_4(t). \end{aligned} \right\} \quad (3.1)$$

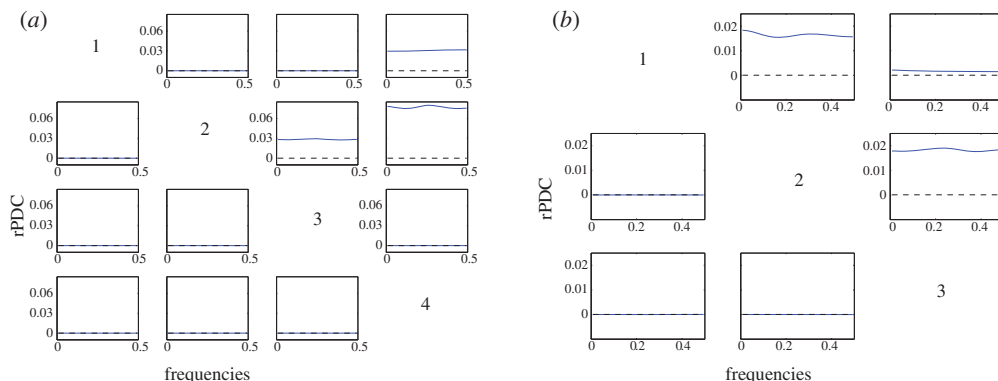


Figure 1. (a) The results of the rPDC estimation based on simulated data of the four-dimensional VAR process of order 2 given by equation (3.1). Each subfigure contains the result of an individual rPDC estimation, such that the results from the component corresponding to the column number to the component corresponding to the row number is shown. (b) The results of the rPDC estimation when the time-series data of the fourth component is disregarded. (Online version in colour.)

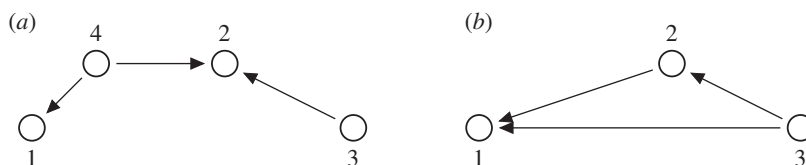


Figure 2. The associated Granger causality graph of the four-dimensional VAR is depicted in (a), and the associated graph when the fourth component is disregarded is shown in (b).

Data that comprise the autoregressive structure above with fixed values of $\alpha = 0.5$, $\beta = 0.8$ and $\gamma = 0.4$ were generated. A VAR process was fitted to 100 000 simulated data points using the maximum-likelihood method.

Results of the rPDC analysis are shown in figure 1, where dashed lines indicate significant levels. Using the rPDC estimation, values that are significantly non-zero entail edges in the associated graph (figure 2). Significant directed influences are present from the fourth to both the first and the second component, as well as from the third to the second component. The simulation and subsequent estimation of the connectivity structure confirmed the generated interdependencies.

Owing to incomplete data acquisition or owing to preprocessing of the data, important components of a system could be disregarded. Consider a subsystem in which one of the four components was left out. In this case, some influences on the system are unobserved, and the considered subsystem is affected by latent sources. To study such an exclusion of an important component, the fourth component of the introduced system is now disregarded in the data analysis.

The estimation of renormalized PDCs performed for the three time series is depicted in figure 1b. Significantly, non-zero values are evident from the third to the second and from the second to the first component, as well as from the third to the first component. This results in figure 2b.

The indirect interrelation between component X_1 and X_2 , which is mediated by component X_4 , becomes a direct relation from component X_2 to component X_1 . Additionally, another directed edge is contained in the graph owing to the latent influence of the fourth component. Through the direct linkage from X_2 to X_1 , together with the preceding direct influence of X_3 to X_2 , a new directed edge originates that shows a direct impact of component X_3 on component X_1 . This shows that not only trivial but also unforeseen connectivities arise in analyses impacted by latent sources.

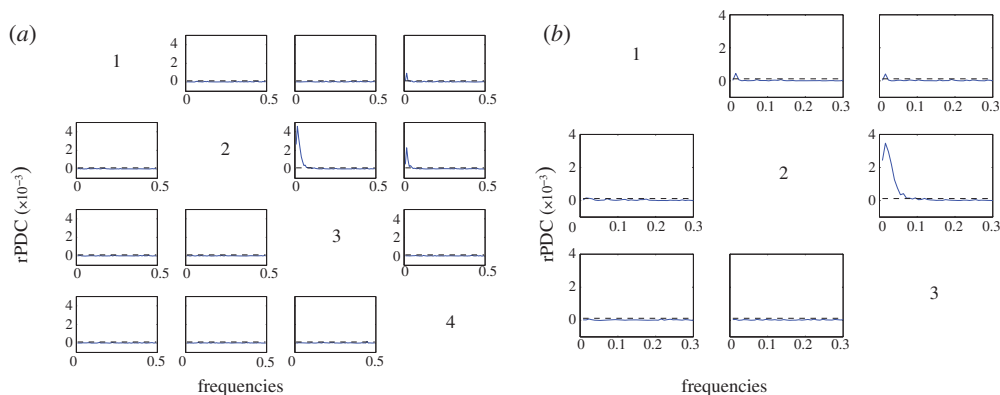


Figure 3. (a) The results of the rPDC analysis of the nonlinear system consisting of four coupled Roessler systems. Direct influences from component four to components one and two, as well as direct influences from component three to component two, are detected. (b) The results, when the fourth Roessler component is unobserved. Directed connections from component three to components one and two are detected, as well as a direct connection from component two to component one. (Online version in colour.)

(b) Analysis of a nonlinear system

Although the derivation of directed graphs using renormalized PDC constitutes a multivariate analysis tool that relies on linear methods, it may be applied in the nonlinear context as well. For various systems, investigations revealed that linear methods are also applicable in the nonlinear case, but without concluding in a universal concept. For Roessler systems and related ones, see [39,40]. The following analysis of the effect of latent confounders in the context of a Roessler system underpins the crucial impact of unobserved components in this nonlinear context.

In order to establish an equivalent starting point as in the linear case, a network of four coupled Roessler systems is used with the same interaction structure as in the linear example in §3a. Data of the complex system are generated according to the following equations:

$$\left. \begin{aligned} \dot{x}_k &= -(\omega_k y_k + z_k) + \alpha_{k1}(x_1 - x_k) + \dots + \alpha_{k4}(x_4 - x_k) + \varepsilon_k, \\ \dot{y}_k &= \omega_k x_k + a y_k \\ \text{and} \quad \dot{z}_k &= b + z_k(x_k - c), \end{aligned} \right\} \quad (3.2)$$

for $k = 1, \dots, 4$. The parameters are $\omega_1 = 1.03$, $\omega_2 = 0.97$, $\omega_3 = 1.09$, $\omega_4 = 0.91$, $a = 0.15$, $b = 0.2$, $c = 10$, $\alpha_{14} = 0.4$, $\alpha_{23} = 0.5$, $\alpha_{24} = 0.5$ and $\alpha_{kl} = 0$ otherwise. The results of the rPDC analysis are depicted in figure 3. As in the linear case, rPDC analysis is performed and repeated, disregarding the data generated from the fourth component. This leads to the results shown in figure 3b.

The rPDC analysis of the nonlinear system also reveals the impact of latent confounders leading to falsely derived edges. The shown numerical evidence suggests that the investigation in the linear context may be further transferred to nonlinear cases.

4. Three types of influence paths

Renormalized PDC is a multivariate analysis tool, i.e. all other components are taken into account in the analysis of the interrelation between a pair of components. In bivariate analyses, pairs of components are investigated without considering other components. For three components, the bivariate analysis coincides with an analysis of a two-dimensional subsystem with one latent

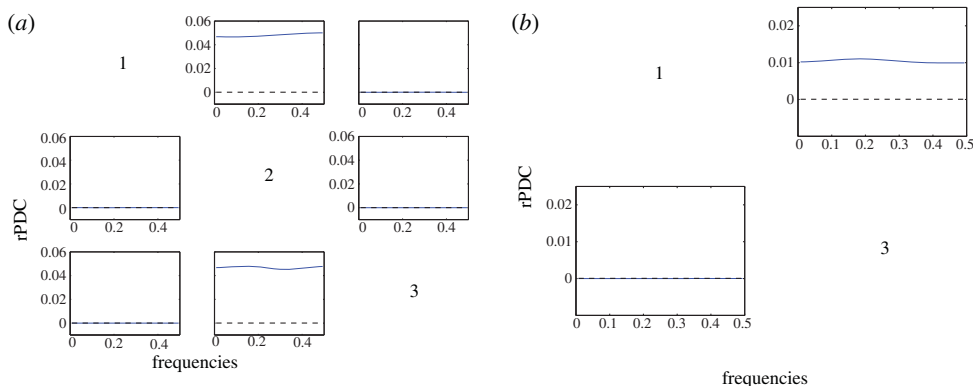


Figure 4. The multivariate rPDC analysis of the data generated by the autoregressive process for the directed path of type 1. The directed influence from component two to components one and three is confirmed by the analysis in (a). The bivariate analysis of component one and three is depicted in (b). (Online version in colour.)

confounder. For a stationary stochastic process with three components X_1 , X_2 and X_3 , consider the following three basic types of paths between X_1 and X_3 :

type 1: $X_1 \leftarrow X_2 \rightarrow X_3$, **type 2:** $X_1 \rightarrow X_2 \leftarrow X_3$ and **type 3:** $X_1 \rightarrow X_2 \rightarrow X_3$.

To better understand the impact of latent confounders, the three basic types of paths of directed influences within a set of three components, i.e. fork, inverted fork and chain, are studied in the introduced linear and nonlinear systems. Effects in basic paths further provide insights for more complicated structures, which can be expressed as combinations of basic paths.

(a) Type 1 (fork)

For the directed path of type 1, time-series data were generated according to the autoregressive representation

$$X_1(t) = \alpha X_2(t-2) + \varepsilon_1(t), \quad X_2(t) = \varepsilon_2(t) \quad \text{and} \quad X_3(t) = \alpha X_2(t-1) + \varepsilon_3(t),$$

where $\alpha = 0.5$ was chosen. Note that the time lags differ such that the influences of component X_2 on both other components are not the same.

The same structure is realized in a coupled Roessler system based on the equations of §3b (equations (3.2)), but for $k = 1, \dots, 3$, and with parameters $\omega_1 = 1.01$, $\omega_2 = 1.03$, $\omega_3 = 0.99$, $a = 0.15$, $b = 0.2$, $c = 10$, $\alpha_{12} = 0.1$, $\alpha_{32} = 0.15$ and $\alpha_{kl} = 0$ otherwise. Performance of the rPDC estimation for both systems yields the connectivity structure as expected (figures 4a and 5a), and the resulting graphs contain two directed edges: a directed edge from component X_2 to X_1 and another directed edge from component X_2 to X_3 (figure 6a).

Next, alterations of interrelations between pairs of components are studied, when the intermediate component is unobserved. Therefore, the rPDC estimation is repeated three times and each time, one of the time-series data is left out. If directly linked pairs are considered, the expected result should comprise a direct linkage as well. More interesting is the case of disregarding component X_2 . In this case, X_2 constitutes a latent confounder that influences both components under investigation. Every single bivariate analysis yields one graph with two vertices. For better comparison, the three graphs of the three analyses are combined into one graph, where the same vertices are identified. Because the results depict bivariate considerations, the combined graphs are referred to as *bivariate graphs* as in [2], and dashed directed edges are used.

In figures 4b and 5b, results of the bivariate rPDC analysis for components one and three are displayed for each system, respectively. As the rPDC analysis shows, a direct influence is found

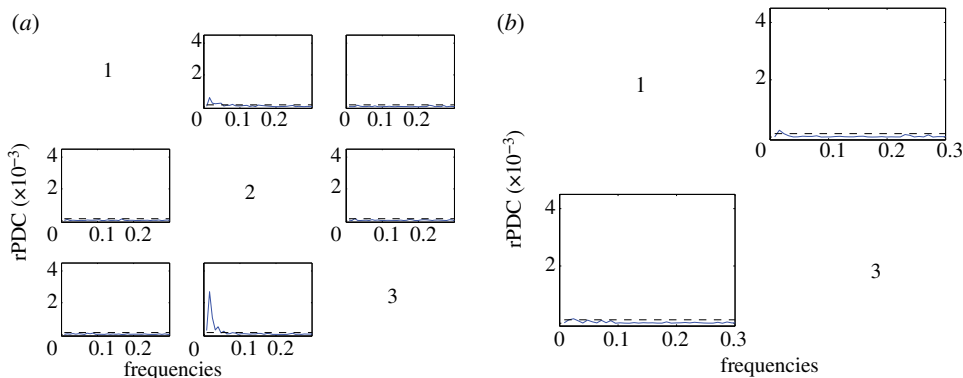


Figure 5. The multivariate rPDC analysis of the data generated by the coupled Roessler system for the directed path of type 1. In (a), the analysis of all three components is displayed and in (b), the bivariate analysis of component one and three is shown. (Online version in colour.)



Figure 6. The graph associated with the multivariate analysis of influence type 1 is shown in (a). In (b), the corresponding bivariate graph is depicted.

from component X_2 to components X_1 and X_3 , as well as a direct influence from component X_3 to component X_1 . This results in the bivariate graph shown in figure 6b. The bivariate graph contains an additional directed edge between the first and third components. Thus, if the second component would have been unobserved, a direct influence from the third to the first component would have been perceived.

(b) Type 2 (inverted fork)

The same procedure is performed for type 2. In the linear case, time-series data were generated according to the VAR process

$$X_1(t) = \varepsilon_1(t), \quad X_2(t) = \alpha X_1(t-1) + \beta X_3(t-2) + \varepsilon_2(t) \quad \text{and} \quad X_3(t) = \varepsilon_3(t),$$

with values $\alpha = 0.5$ and $\beta = 0.8$. In the nonlinear case, the coupled Roessler system (equation (3.2)) was realized for $k = 1, \dots, 3$, $\omega_1 = 1.01$, $\omega_2 = 1.03$, $\omega_3 = 0.99$, $a = 0.15$, $b = 0.2$, $c = 10$, $\alpha_{21} = 0.1$, $\alpha_{23} = 0.1$ and $\alpha_{kl} = 0$ otherwise.

As in §4a, rPDC analyses for the complete sets of time-series data result in graphs containing edges according to the desired directed influences. Then, rPDC analysis is performed for all pairs of components separately, in order to derive bivariate graphs.

Results for the nonlinear system are displayed in figure 7. Figure 8 depicts the multivariate and bivariate graphs for the influence path of type 2 obtained by both systems. In pathways of type 2, both graphs are the same, which implies that no additional structure arises, if component two is unobserved.

(c) Type 3 (chain)

The last type of influence path is studied via generated data from the autoregressive model

$$X_1(t) = \varepsilon_1(t), \quad X_2(t) = \beta X_1(t-1) + \varepsilon_2(t) \quad \text{and} \quad X_3(t) = \alpha X_2(t-2) + \varepsilon_3(t),$$

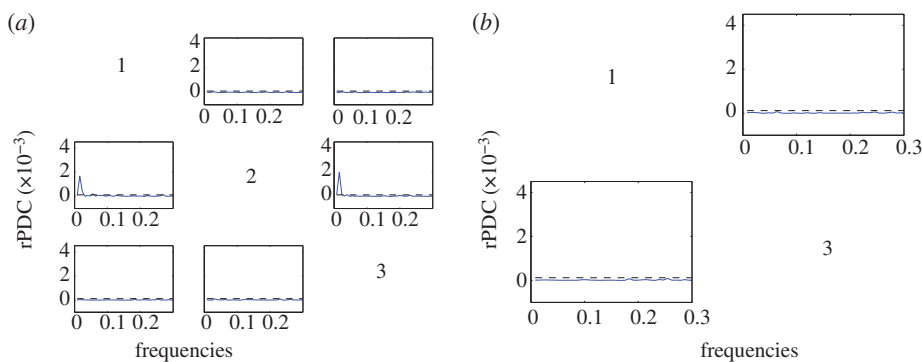


Figure 7. The multivariate rPDC analysis of the nonlinear time-series data for the directed path of type 2 in (a), and the bivariate analysis of components one and three in (b). (Online version in colour.)



Figure 8. The graph of the multivariate analysis is displayed in (a). (b) The bivariate graph, which in this case shows no effect of latent sources.



Figure 9. The graph of the multivariate analysis in (a) versus the bivariate graph in (b), in the case of type 3.

where $\alpha = 0.5$ and $\beta = 0.8$, and the coupled Roessler system obtained as in equation (3.2), for $k = 1, \dots, 3$, $\omega_1 = 1.01$, $\omega_2 = 0.99$, $\omega_3 = 0.97$, $a = 0.15$, $b = 0.2$, $c = 10$, $\alpha_{21} = 0.15$, $\alpha_{32} = 0.1$ and $\alpha_{kl} = 0$ otherwise. Moreover, the analysis was additionally performed in the nonlinear case for the same parameters, but $\alpha_{12} = 0.1$ and $\alpha_{21} = 0.1$, in order to also study a system with a reciprocal directed connection.

Again, rPDC analysis, performed for all three time-series datasets, yields a graph that contains the influence path as intended. Moreover, the executed bivariate subanalyses for all pairs of components result in the combined bivariate graph. Figure 9 contains both graphs, i.e. from multivariate and bivariate considerations, in the case of type 3. The additional reciprocal connection resulted in an additional edge from vertex 2 to vertex 1, as can be seen from the results of the analysis in figure 10. Here, the bivariate graph again contains an additional edge between components one and three. This edge is due to the unobserved intermediate components, i.e. the second component. In such influence pathways, a spurious direct edge would have been derived.

In summary, the pairwise investigation revealed that in the case of type 1 (fork) and type 3 (chain), bivariate graphs differ from the graphs derived in multivariate analysis. Both bivariate graphs contain an additional edge between the first and the third component. In the case of type 1,

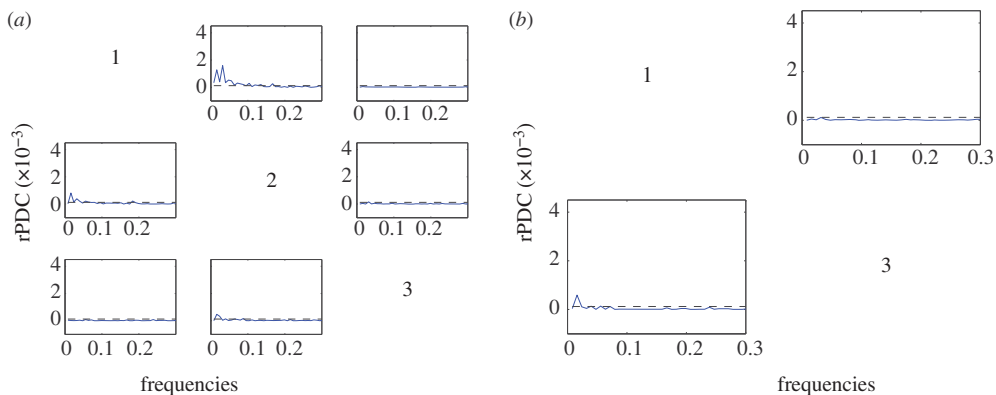


Figure 10. The rPDC analysis of the nonlinear system containing an additional reciprocal connection for all components (a) and components one and three (b). (Online version in colour.)

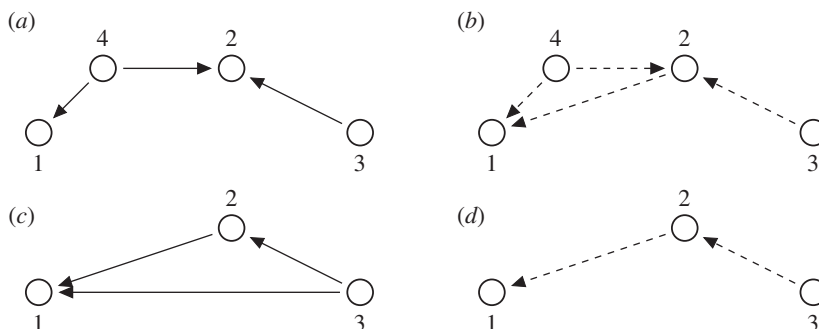


Figure 11. The associated graph of the initial four-dimensional VAR in (a), together with its corresponding bivariate graph in (b). Associated multivariate and bivariate graphs for the subsystem of three components, where component four is disregarded are shown in (c) and (d).

the direction of the additional edge is determined by the difference of time lags of the unobserved component's influence. In influence type 2, no additional edge occurs. In all three cases, the graph of multivariate considerations is a subgraph of the bivariate graph.

5. Multiple renormalized partial directed coherence analysis

The edges in bivariate graphs reflect connections derived under the premise that all other components were unobserved. This procedure is now applied for the initially studied system given by equation (3.1) and further for its subsystem affected by one latent confounder. According to the results from §4c, latent confounders in paths of type 1 (fork) and 3 (chain) led to additional direct connections.

The associated graph in the multivariate analysis and the derived bivariate graph of the four-dimensional VAR process given by equation (3.1) are depicted next to each other in figure 11a,b. In addition, for the three-dimensional subsystem, where the fourth component is unobserved, a bivariate graph is derived. The resulting graphs are shown in figure 11a,b. It is striking that in the analysis of the not fully observed system, the multivariate graph is *not* a subgraph of the bivariate graph. There is no dashed directed edge between vertex 3 and vertex 1 because in the original graph, both vertices are neither connected via a fork nor chain. In this way, the combination of multivariate considerations, together with an additional bivariate analysis,

can support the substantiation of influence assertions. However, to obtain overall assertions, all possible subsystems have to be analysed.

6. Consequences for applications

As demonstrated in the previous sections, missing important components of a network in the analysis might eventually result in spurious interactions. Missing important components are certainly one of the problems most often faced. In studies based on EEG recordings [41], the typical scenario is to have either scalp electrodes or invasive electrodes covering certain brain regions. It is impossible to have electrodes in all potentially interesting brain regions in human studies [42]. In animal studies, this might be possible, although owing to restrictions in the recording equipment and lack of detailed knowledge of potentially interesting brain regions, it is not even expected in animal studies to have a full coverage of these regions. Similar challenges arise in some imaging studies such as NIRS studies [43], in which only a very restricted region of the brain can be observed.

fMRI [23] or MEG [44] studies present an important alternative to standard EEG or NIRS approaches, as these recording entities promise a full coverage of the brain. Still, in these cases, aggregation over spatial information and over time leads to an identification of components that allow latent influences to disturb deriving overall causalities.

Very often, another factor potentially leads to latent variables. Owing to recording capabilities with several hundreds of channels in the measurement space that potentially observe a similar amount of sources of activity, a reduction in the dimensionality is a necessary first step in the analysis. Without such a reduction, most multivariate analysis techniques are simply not feasible owing to numerical complexity or problems with numerical stability. For instance, most methods for directional connectivity are based on fitting of unconstrained VAR models, which becomes infeasible for large dimensions owing to the very large number of parameters.

In Granger causality analyses, the effect of potentially important third but latent processes is often ignored. Only in a very few studies, is it clearly mentioned that the Granger causality network obtained is restricted to the observations made, as originally emphasized by Granger [19]. Causal inference has only recently become a topic of interest. Causal inference refers to the investigation of the true underlying network structure based on limited observations. As demonstrated in the previous sections, in some cases, this is indeed possible using subnetwork analysis. In future applications of Granger causality analysis, the potential role of latent variables should be thoroughly addressed and, potentially, the advanced information contained in subnetwork analysis should be explored.

7. Discussion

Stochastic processes as they occur in natural procedures are often very complex, and measurements mostly cover only parts of the complex process. Moreover, owing to the complexity of acquired data, it is necessary to select a subset of components for application of multivariate analysis techniques. However, selection of components for a causality analysis is a preprocessing step that includes predetermined exclusion of information, which generates latent confounders.

In the context of partial coherence [31], falsely detected influence between two components, caused by a third component, occurs if both exhibit a connection to a common third component. This effect is referred to as *marrying parents of a joint child* [1,45]. In theoretical causality considerations, a similar effect is known under the term *spurious causality of type one*, which indicates causalities that appear in the full system and disappear in smaller subsystems as discussed by [46]. In the context of Granger causality graphs, the knowledge of the effects of one latent component in simple networks consisting of three components can potentially be used to predict the impact of latent confounders in larger networks. Directed influences of components that are missing in the analysis is sort of dispersed to the remaining observed components, and the alterations induced by a latent confounder further affect relations between components

that are not directly linked to the latent confounder. If additional background knowledge about the underlying process supports the investigation, then such assertions could be decisive in the determination of connectivity structures.

In the case of marrying parents of a joint child, bivariate analysis, i.e. coherence instead of partial coherence, could sometimes be used to investigate such false connections. In the context of Granger causality, bivariate graphs contain edges that are derived with regard to all pairs of time series. If both types of graphs are derived, edges that are contained in both graphs are confirmed with respect to all other components and when dealing just with the two components. These edges ought to depict confirmed directed influences. Edges that are contained only in the bivariate graph, but not in the multivariate graph, indicate derived edges on account of the lack of distinction between direct influences. Direct influence means one component affects the other component directly, and indirect influences are present if one component affects the other component via a path of direct influences. However, if edges appear only in the multivariate graph, but not in the bivariate graph, the analysis may be influenced by latent confounders. In the rather unlikely case that two influence paths occur between two components, such that both paths completely neutralize each other, the bivariate graph may drop an edge that is contained in the multivariate graph. Nevertheless, such neutralizing doubled paths in complex systems that arise in nature are doubtful.

8. Conclusion

In this article, the impact of latent confounders was demonstrated, and the problem of arbitrariness in choosing and aggregating components for the investigation addressed. The occurrence of additional spurious edges, owing to unobserved influences of latent confounders, was simulated in the linear and nonlinear case. In order to classify the impact of latent confounders, influence pathways among three components were considered in simulations. Pairwise considerations of paths with three components revealed that additional directed edges occur following influence paths of type 1 (fork) and type 3 (chain). In influence paths of type 2 (inverted fork), no additional edge occurs. The combination of multivariate and bivariate analysis, in addition to further subanalyses, in dealing with latent confounders was suggested to give evidence for unobserved components that affected the network under consideration. All analyses were performed using rPDC estimation as a measure of Granger causality in the frequency domain; the problem of latent confounding, however, is not bound to the chosen measure but appears generally.

Granger causality is applicable in neuroscience, but with potential problems due to latent confounding, as we demonstrate in our work. Therefore, latent confounders require further research and experimental validation in order to be able to deal with the effects within the analysis. Most important is, however, to be aware of the effects that unobserved or excluded components have within the analysis.

References

1. Dahlhaus R, Eichler M, Sandkühler J. 1997 Identification of synaptic connections in neural ensembles by graphical models. *J. Neurosci. Methods* **77**, 93–107. (doi:10.1016/S0165-0270(97)00100-3)
2. Eichler M. 2005 A graphical approach for evaluating effective connectivity in neural systems. *Phil. Trans. R. Soc. B* **360**, 953–967. (doi:10.1098/rstb.2005.1641)
3. Friston KJ, Harrison L, Penny W. 2003 Dynamic causal modelling. *NeuroImage* **19**, 1273–1302. (doi:10.1016/S1053-8119(03)00202-7)
4. Schreiber T. 2000 Measuring information transfer. *Phys. Rev. Lett.* **85**, 461–464. (doi:10.1103/PhysRevLett.85.461)
5. Smirnov D, Bezruchko B. 2003 Estimation of interaction strength and direction from short and noisy time series. *Phys. Rev. E* **68**, 046209. (doi:10.1103/PhysRevE.68.046209)

6. Broyd SJ, Demanuele C, Debener S, Helps SK, James CJ, Sonuga-Barke EJS. 2009 Default-mode brain dysfunction in mental disorders: a systematic review. *Neurosci. Biobehav. Rev.* **33**, 279–296. (doi:10.1016/j.neubiorev.2008.09.002)
7. Bullmore E, Sporns O. 2009 Complex brain networks: graph theoretical analysis of structural and functional systems. *Nat. Rev. Neurosci.* **10**, 186–198. (doi:10.1038/nrn2575)
8. Damoiseaux JS, Greicius MD. 2009 Greater than the sum of its parts: a review of studies combining structural connectivity and resting-state functional connectivity. *Brain Struct. Funct.* **213**, 525–533. (doi:10.1007/s00429-009-0208-6)
9. Dosenbach NUF *et al.* 2010 Prediction of individual brain maturity using fMRI. *Science* **329**, 1358–1361. (doi:10.1126/science.1194144)
10. Zhang DY, Raichle ME. 2010 Disease and the brain's dark energy. *Nat. Rev. Neurol.* **6**, 15–28. (doi:10.1038/nrneurol.2009.198)
11. Smith SM, Miller KL, Salimi-Khorshidi G, Webster M, Beckmann CF, Nichols TE, Ramsey JD, Woolrich MW. 2011 Network modelling methods for fMRI. *NeuroImage* **54**, 875–891. (doi:10.1016/j.neuroimage.2010.08.063)
12. Berzuini C, Dawid AP, Bernardinelli, L. (eds) 2012 *Causality: statistical perspectives and applications*. London, UK: Wiley.
13. Pearl J. 2009 *Causality*, 2nd edn. Cambridge, UK: Cambridge University Press.
14. Eichler M. 2013 Causal inference in time series analysis. In *Causality: statistical perspectives and applications* (eds C Berzuini, AP Dawid & L Bernardinelli), pp. 327–354. London, UK: Wiley.
15. Eichler M. 2013 Causal inference with multiple time series: principles and problems. *Phil. Trans. R. Soc. A* **371**, 20110613. (doi:10.1098/rsta.2011.0613)
16. Chicharro D, Ledberg A. 2012 When two become one: the limits of causality analysis of brain dynamics. *PLoS ONE* **7**, e32466. (doi:10.1371/journal.pone.0032466)
17. Eichler M, Didelez V. 2010 On Granger causality and the effect of interventions in time series. *Lifetime Data Anal.* **16**, 3–32. (doi:10.1007/s10985-009-9143-3)
18. Valdes-Sosa PA, Roebroeck A, Daunizeau J, Friston K. 2011 Effective connectivity: influence, causality and biophysical modeling. *NeuroImage* **58**, 339–361. (doi:10.1016/j.neuroimage.2011.03.058)
19. Granger CWJ. 1969 Investigating causal relationships by econometric models and cross-spectral methods. *Econometrica* **37**, 424–438. (doi:10.2307/1912791)
20. Granger CWJ. 1980 Testing for causality. *J. Econ. Dyn. Control* **2**, 329–352. (doi:10.1016/0165-1889(80)90069-X)
21. Granger CWJ. 1988 Some recent developments in a concept of causality. *J. Econ.* **39**, 199–211. (doi:10.1016/0304-4076(88)90045-0)
22. Mader W, Feess D, Lange R, Saur D, Glauche V, Weiller C, Timmer J, Schelter B. 2008 On the detection of direct directed information flow in fMRI. *IEEE J. Selected Top. Signal Process.* **2**, 965–974. (doi:10.1109/JSTSP.2008.2008260)
23. Roebroeck A, Formisano E, Goebel R. 2005 Mapping directed influence over the brain using Granger causality and fMRI. *NeuroImage* **25**, 230–242. (doi:10.1016/j.neuroimage.2004.11.017)
24. Eichler M. 2007 Granger causality and path diagrams for multivariate time series. *J. Econ.* **137**, 334–353. (doi:10.1016/j.jeconom.2005.06.032)
25. Eichler M. 2011 Graphical modelling of multivariate time series. *Prob. Theory Related Fields* **149**, 233–268. (doi:10.1007/s00440-011-0345-8)
26. Bialonski S, Horstmann M, Lehnertz K. 2010 From brain to earth and climate systems: small-world interaction networks or not? *Chaos* **20**, 013134. (doi:10.1063/1.3360561)
27. Guo S, Seth AK, Kendrick KM, Zhou C, Feng, J. 2008 Partial Granger causality: eliminating exogenous inputs and latent variables. *J. Neurosci. Methods* **172**, 79–93. (doi:10.1016/j.jneumeth.2008.04.011)
28. Porta A, Bassani T, Bari V, Pinna GD, Maestri R, Guzzetti S. 2012 Accounting for respiration is necessary to reliably infer Ganger causality from cardiovascular variability series. *IEEE Trans. Biomed. Eng.* **59**, 832–841. (doi:10.1109/TBME.2011.2180379)
29. Pearl J. 1992 A statistical semantics for causation. *Stat. Comput.* **2**, 91–95. (doi:10.1007/BF01889587)
30. Borgelt C, Kruse R. 1999 A critique of inductive causation. In *Symbolic and quantitative approaches to reasoning and uncertainty* (eds A Hunter, S Parsons), pp. 68–79. Berlin, Germany: Springer.

31. Schelter B, Timmer J, Eichler M. 2009 Assessing the strength of directed influences among neural signals using renormalized partial directed coherence. *J. Neurosci. Methods* **179**, 121–130. (doi:10.1016/j.jneumeth.2009.01.006)
32. Baccalá LA, Sameshima K. 2001 Partial directed coherence: a new concept in neural structure determination. *Biol. Cybern.* **84**, 463–474. (doi:10.1007/PL00007990)
33. Sameshima K, Baccalá LA. 1999 Using partial directed coherence to describe neuronal ensemble interactions. *J. Neurosci. Methods* **94**, 93–103. (doi:10.1016/S0165-0270(99)00128-4)
34. Brockwell PJ, Davis RA. 1991 *Time series: theory and methods*. Berlin, Germany: Springer.
35. Eichler M. 2006 Graphical modeling of dynamic relationships in multivariate time series. In *Handbook of time series analysis* (eds B Schelter, M Winterhalder, J Timmer), pp. 335–372. London, UK: Wiley-VCH.
36. Lütkepohl H. 2006 *New introduction to multiple time series analysis*. Berlin, Germany: Springer.
37. Lauritzen SL. 1996 *Graphical models*. Oxford Statistical Science Series, vol. 17. Oxford, UK: Oxford Science Publications.
38. Dahlhaus R. 2000 Graphical interaction models for multivariate time series. *Metrika* **51**, 157–172. (doi:10.1007/s001840000055)
39. Jachan M, Henschel K, Nawrath J, Schad A, Timmer J, Schelter B. 2009 Inferring direct directed information flow from multivariate non-linear time series. *Phys. Rev. E* **80**, 011138. (doi:10.1103/PhysRevE.80.011138)
40. Sommerlade L, Eichler M, Jachan M, Henschel K, Timmer J, Schelter B. 2009 Estimating causal dependencies in networks of nonlinear stochastic dynamical systems. *Phys. Rev. E* **80**, 051128. (doi:10.1103/PhysRevE.80.051128)
41. Nunez PL, Srinivasan R. 1981 *Electric fields of the brain: the neurophysics of EEG*. Oxford, UK: Oxford University Press.
42. Bernasconi C, König P. 1999 On the directionality of cortical interactions studied by structural analysis of electrophysiological recordings. *Biol. Cybern.* **81**, 199–210. (doi:10.1007/s004220050556)
43. Jobsis FF. 1977 Noninvasive infrared monitoring of cerebral and myocardial sufficiency and circulatory parameters. *Science* **198**, 1264–1267. (doi:10.1126/science.929199)
44. Timmermann L, Gross J, Dirks M, Volkmann J, Freund HJ, Schnitzler A. 2003 The cerebral oscillatory network of parkinsonian resting tremor. *Brain* **126**, 199–212. (doi:10.1093/brain/awg022)
45. Eichler M, Dahlhaus R, Sandkühler J. 2003 Partial correlation analysis for the identification of synaptic connections. *Biol. Cybern.* **89**, 289–302. (doi:10.1007/s00422-003-0400-3)
46. Hsiao C. 1982 Autoregressive modeling and causal ordering of econometric variables. *J. Econ. Dyn. Control* **4**, 243–259. (doi:10.1016/0165-1889(82)90015-X)